

The Effect Of Rotor And Stator Slot Numbers On The Performance Of Three-Phase Induction Motors Used For Transport Application

Asuquo Eke, Gertrude Fischer, Ake David, Okon Ekpenyong, Akpama E.J.,
Department Of Electrical/Electronic Engineering
Cross River State University, Calabar. Nigeria

Abstract

Modeling and design of the induction motor were done with a reference frame approach, spacing of rotor slots has a significant effect on an induction motor. Correct selection of a number of rotor bars in relation to pole pairs and quantity of stator slots. A poor design choice on this section of the machine could result in unsustainable torques in the finished product. Designing is the act of deciding the actual dimensions of the motor parts and components that constitute the motor. This was done by employing the FEM method and it was implemented using motor cad. Two motors were designed having the same parameters with a difference in rotor/stator slot numbers 24/26, and 28/36 only. This was done to determine the impact of the stator and rotor slot number on the motor performance. The results reveal that design1 has an efficiency of 88.5 % while motor design2 has 72.8%. a high starting torque was discovered in motor design1 with a small settling time of 0.115 seconds. Motor design 2 has a high starting current of at a time 0.0225 seconds and also, motor design 2 has a higher power capacity of 12,000W when compared to 8000W of motor design1.

Keywords: Motor Performance, Rotor, Stator, Slot Number, Effects and Transport Applications.

Date of Submission: 08-07-2024

Date of acceptance: 18-07-2024

I. Introduction

The number of rotor slots and stator slots are two significant design characteristics that affect the performance of a three-phase induction motor. Look at how these elements affect the motor's performance. The rotor slots are the apertures on the rotor's surface where the rotor windings are located. The number of rotor slots has an immediate impact on the characteristics of motor performance. An induction motor with more rotor slots has a larger starting torque. This is because a greater number of slots results in a more distributed and balanced rotor winding, resulting in a higher efficiency. Synchronous Speed: The number of rotor slots determines the motor's synchronous speed. A motor with more slots may have a somewhat lower synchronous speed than a motor with fewer slots. Motors with many number of rotor slots have lower torque ripple, resulting in smoother operation and less mechanical stress on the motor. The stator slots are the apertures on the stator that house the stator windings. The number of stator slots has the following effects on motor performance. The number of stator slots influences the presence of harmonics in the magnetic field of the motor. An incorrect selection of stator slot numbers might result in increased harmonics, resulting in greater losses. The spatial distribution of the magnetic field and the associated torque generation are influenced by the stator slot arrangement. The appropriate selection of stator slot numbers can increase motor efficiency and optimize torque production. The design of the stator slot has a direct impact on the motor's noise and vibration levels during operation. A careful choice of slot numbers can result in a quieter and smoother motor operation. The form and quantity of stator slots affect the cooling effectiveness of the motor. Adequate cooling is required to avoid overheating and ensure proper motor functioning. Overall, both the rotor and stator slot numbers are important in influencing the performance of a three-phase induction motor. A well-balanced combination of these factors, coupled with other design considerations, can result in a high-performance, energy-efficient motor. However, motor design is a difficult process with several trade-offs, and an in-depth analysis is required to arrive at the best configuration for certain applications. [1,4,6,10]

Induction motor rotor slots are responsible for enclosing the rotor windings. Several performance characteristics are affected by the number of rotor slots. Number of rotor slots determines the motor's starting torque. The higher the number of rotor slots, the greater the initial torque. This is because additional rotor slots provide higher rotor performance. Torque Ripple is affected by the number of rotor slots, which relates to the change in torque during each revolution. A greater number of rotor slots aids in torque ripple reduction, resulting in smoother motor operation. The number of rotor slots selected can affect the motor's efficiency. Optimal slot

numbers can reduce rotor resistance, leakage reactance, and rotor current losses. Improper rotor slot number selection may result in higher noise and vibration levels. Higher harmonics present in the air gap magnetic field can cause auditory noise and mechanical vibrations. In a three-phase induction motor, the stator number refers to the number of stator windings or phases. The winding configuration of the stator. The stator windings generate the necessary spinning magnetic field for motor operation. Increasing the stator phases (for example, from three to six) can result in a more sinusoidal and smooth magnetic field distribution, which reduces harmonics and improves motor performance. The number of stator windings influences the starting torque of the motor. Additional stator windings can improve starting torque, which is useful in applications requiring strong starting torque. Efficiency is influenced by the stator winding configuration. A well-designed stator winding arrangement can reduce copper losses and increase power factor, resulting in increased efficiency. The harmonic content of the motor's input current is affected by the number of stator phases. Increasing the phases of the stator can aid in the reduction of harmonic distortion. It's vital to remember that choosing rotor slot numbers and stator winding topologies includes trade-offs and the best design is determined by the unique application requirements, such as required torque, efficiency, starting performance, and cost concerns. To identify the best combination of slot numbers and stator windings for a specific motor design, extensive analytical and simulation approaches are often used. A three-phase induction motor's rotor and stator slot count can have a considerable impact on its performance and features. Here's how each parameter influences how the motor behaves. The number of rotor slots influences the motor's starting and running torque. An optimal number of rotor slots aids in the generation of increased torque at low speeds, as well as the improvement of the motor's starting capabilities. Cogging torque is a pulsing torque produced when the rotor of a motor aligns with the stator slots. A mismatch in the number of rotor slots and stator slots can cause cogging torque to be reduced or increased, resulting in unwanted vibrations and noise. Increased rotor slot count can result in higher rotor losses due to increased eddy current and hysteresis losses. The synchronous speed of the motor is determined by the stator slot number. The revolving magnetic field produced by the stator winding rotates at a synchronous speed. Synchronous Speed (rpm) = $(120 * \text{Frequency}) / \text{Number of Stator Slots}$ is the formula. The number of stator slots influences the harmonic content of the air gap magnetic field in the motor. either too few or too many stator slots can increase harmonics and produce more noise in the motor operation. The starting torque and torque ripple characteristics of the motor are influenced by the stator slot number. A higher stator slot number might result in smoother torque production and improved starting performance. Overall, the rotor and stator slot designs are critical in optimizing the performance of a three-phase induction motor. It involves a trade-off of several aspects, such as starting torque, operating efficiency, cogging torque, and noise. Proper rotor and stator slot selection and design are critical for achieving the necessary motor performance for certain applications. To fine-tune these characteristics based on the motor's intended application and load requirements, computer simulations and prototyping are frequently used. [12,14]

Proper selection of stator slot numbers can lead to a higher power factor, which is desirable for efficient power utilization. The choice of stator slot numbers can influence torque ripple. Minimizing torque ripple enhances motor smoothness and reduces mechanical stress on the motor and driven machinery. The number of stator slots can impact the motor's starting performance, affecting its ability to produce sufficient torque during start-up. It is essential to strike a balance between the number of rotor and stator slots, taking into account various

In practical motor design, engineers consider a range of factors, including material properties, manufacturing constraints, electromagnetic considerations, and economic factors to arrive at the best compromise between efficiency, performance, and cost-effectiveness for a particular application. The performance of a three-phase induction motor is influenced by several factors, including the number of rotor slots and stator slots. Both these factors can affect the motor's efficiency, power factor, starting torque, and overall operating characteristics. Let's look at each one separately. The number of rotor slots in an induction motor influences its starting torque, efficiency, and smoothness of operation. Here's how rotor slot numbers impact the motor's performance. [15,17]

More rotor slots generally result in higher starting torque. This is because a higher number of rotor slots provides better torque production capability during motor start-up. A moderate number of rotor slots is often preferred for achieving better efficiency. Too few or too many slots may lead to increased rotor losses, reducing overall efficiency. A higher number of rotor slots can lead to more harmonics and increased noise levels, affecting the motor's acoustic performance. In some cases, uneven distribution of rotor slots, known as rotor skewing, can help reduce torque ripple and improve motor performance. [10, 17.19, 20]

II. Dynamic Model Equation For Three-Phase Induction Machine

The dynamic model equations of the induction motor can be obtained from the dq0 equivalent circuit of the induction motor shown in Figure 3.1, figure 3.2, and Figure 3.3. (TriptiRai and Prashant, 2016).

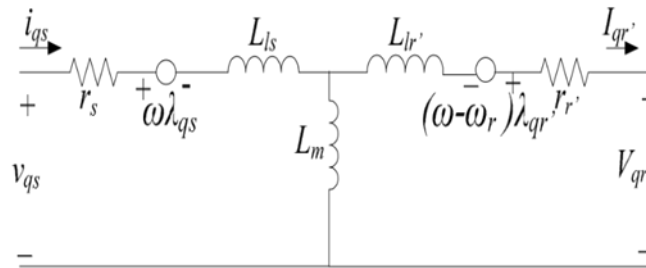


Fig. 1.0: D-axis equivalent circuit of an induction motor.

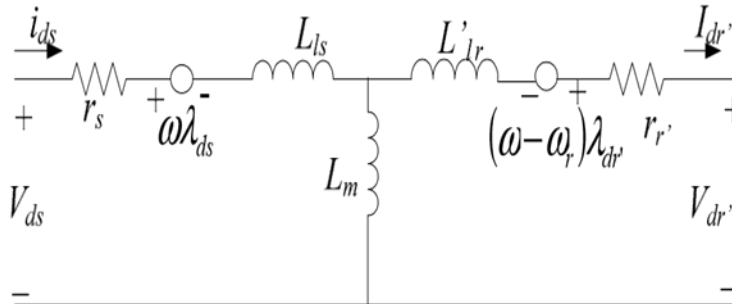


Fig. 2.0: Q-axis equivalent circuit of an induction motor.

Under balanced conditions the three-phase stator voltage of an induction motor can be expressed as equation (1), (2), and (3). [2,5,8, 22]

$$V_a = \sqrt{2} V_{rms} \sin(\omega t) \tag{1}$$

$$V_b = \sqrt{2} V_{rms} \sin\left(\omega t - \frac{2\pi}{3}\right) \tag{2}$$

$$V_c = \sqrt{2} V_{rms} \sin\left(\omega t + \frac{2\pi}{3}\right) \tag{3}$$

These three-phase voltages are transformed into a two-phase synchronously rotating reference frame of dq0 axis. This transformation is achieved through the application of the following transformation matrix as shown in equation (4).

$$\begin{bmatrix} V_\alpha \\ V_\beta \end{bmatrix} = \frac{2}{3} \begin{bmatrix} 1 & \frac{1}{2} & -\frac{1}{2} \\ 0 & \frac{\sqrt{3}}{2} & -\frac{\sqrt{3}}{2} \end{bmatrix} \begin{bmatrix} V_a \\ V_b \\ V_c \end{bmatrix} \tag{4}$$

Then, the dq axis voltages are shown in equation (9):

$$\begin{bmatrix} V_d \\ V_q \end{bmatrix} = \begin{bmatrix} \cos \theta & \sin \theta \\ -\sin \theta & \cos \theta \end{bmatrix} \begin{bmatrix} V_\alpha \\ V_\beta \end{bmatrix} \tag{5}$$

The instantaneous value of the stator and rotor currents of a three-phase induction motor is calculated by using the following matrix equations (6) and (7);

$$\begin{bmatrix} i_\alpha \\ i_\beta \end{bmatrix} = \begin{bmatrix} \cos \theta & -\sin \theta \\ \sin \theta & \cos \theta \end{bmatrix} \begin{bmatrix} i_d \\ i_q \end{bmatrix} \tag{6}$$

$$\begin{bmatrix} i_a \\ i_b \\ i_c \end{bmatrix} = \begin{bmatrix} 1 & 0 \\ \frac{1}{2} & -\frac{\sqrt{3}}{2} \\ -\frac{1}{2} & -\frac{\sqrt{3}}{2} \end{bmatrix} \begin{bmatrix} i_\alpha \\ i_\beta \end{bmatrix} \tag{7}$$

The stator and rotor voltage equation of the direct and quadrature (d-q) axis of an induction motor are given in equations (8), (9), (10), and (11).

$$V_{qs} = R_s i_{qs} + \frac{d}{dt} \lambda_{qs} + \omega_e \lambda_{qr} \tag{8}$$

$$V_{ds} = R_s i_{ds} + \frac{d}{dt} \lambda_{ds} - \omega_e \lambda_{dr} \tag{9}$$

$$V_{qr} = R_r i_{qr} + \frac{d}{dt} \lambda_{qr} + (\omega_e - \omega_r) \lambda_{qr} \tag{10}$$

$$V_{dr} = R_r i_{dr} + \frac{d}{dt} \lambda_{dr} - (\omega_e - \omega_r) \lambda_{dr} \tag{11}$$

Where, λ_{qr} , λ_{qs} , λ_{dr} , and λ_{ds} are the stator and rotor flux linkage of the d and q axis, these equations show the synchronously rotating reference frame for the two-phase d-q-axis of the induction motor.

For squirrel cage induction motor, the rotor voltages V_{qr}, V_{dr} are set to zero, since the rotor cage bars are shorted. Therefore, the flux linkage equation can be expressed as equations (12), (13), (14), (15), (16), (17), and (18). [7, 22, 23]

$$\frac{d\lambda_{qs}}{dt} = \omega_b \left[V_{qs} - \frac{\omega_e}{\omega_b} \lambda_{ds} + \frac{R_s}{X_{ls}} (\lambda_{mq} - \lambda_{qs}) \right] \quad (12)$$

$$\frac{d\lambda_{ds}}{dt} = \omega_b \left[V_{ds} + \frac{\omega_e}{\omega_b} \lambda_{qs} + \frac{R_s}{X_{ls}} (\lambda_{md} - \lambda_{ds}) \right] \quad (13)$$

$$\frac{d\lambda_{qr}}{dt} = \omega_b \left[V_{qs} - \left(\frac{\omega_e - \omega_r}{\omega_b} \right) \lambda_{qr} + \frac{R_r}{X_{lr}} (\lambda_{mq} - \lambda_{qr}) \right] \quad (14)$$

$$\frac{d\lambda_{dr}}{dt} = \omega_b \left[V_{ds} + \left(\frac{\omega_e - \omega_r}{\omega_b} \right) \lambda_{dr} + \frac{R_r}{X_{lr}} (\lambda_{md} - \lambda_{dr}) \right] \quad (15)$$

Where;

$$\lambda_{mq} = X_{ml} \left[\frac{\lambda_{qs}}{X_{ls}} + \frac{\lambda_{qr}}{X_{lr}} \right] \quad (16)$$

$$\lambda_{md} = X_{ml} \left[\frac{\lambda_{ds}}{X_{ls}} + \frac{\lambda_{dr}}{X_{lr}} \right] \quad (17)$$

$$X_{ml} = \frac{1}{\left(\frac{1}{X_m} + \frac{1}{X_{ls}} + \frac{1}{X_{lr}} \right)} \quad (18)$$

To obtain the currents, therefore substitute the value of flux linkages as shown in equations (19), (20), (21), and (22).

$$i_{qs} = \frac{1}{X_{ls}} (\lambda_{qs} - \lambda_{mq}) \quad (19)$$

$$i_{ds} = \frac{1}{X_{ls}} (\lambda_{ds} - \lambda_{md}) \quad (20)$$

$$i_{qr} = \frac{1}{X_{lr}} (\lambda_{qr} - \lambda_{mq}) \quad (21)$$

$$i_{dr} = \frac{1}{X_{lr}} (\lambda_{dr} - \lambda_{md}) \quad (22)$$

Based on the above equations, the torque and rotor speed can be determined as equations (23) and (24).

$$T_e = \frac{3}{2} \left(\frac{p}{2} \right) (\lambda_{qr} i_{dr} - \lambda_{dr} i_{qr}) \quad (23)$$

$$\omega_e = \int \frac{p}{2} (T_e - T_L) \quad (24)$$

III. Motor Design

The stator bore diameter of the SCIM is given according to [18, 21, 24]

$$D_{is(SCIM)} = \sqrt[3]{\frac{2P_1^2 S_{gap}}{\pi \lambda f C_0}}, \quad (25)$$

where pole pairs, apparent airgap power, aspect ratio, supply frequency, and Esson's constant (147×103 J/m³) are represented by the variables p_1 , S_{gap} , λ , f , and C_0 , respectively.

For dimensioning the SCIM, the following formulas are used to get the pole pitch, $\tau(SCIM)$, stack length, $L_{st(SCIM)}$, and slot pitch,

$$\tau_s(SCIM): \tau(SCIM) = \frac{\pi D_{is(SCIM)}}{2p_1}, L_{st(SCIM)} = \lambda \tau(SCIM), \tau_s(SCIM) = \frac{\tau(SCIM)}{3q}. \quad (26)$$

The aspect ratio, pole pitch, and stator slots per pole are respectively represented as λ , $\tau(SCIM)$, and q , whereas the stator outer diameter, $D_{os(SCIM)}$, airgap length, and rotor outer diameter are approximated as follows:

$$D_{os(SCIM)} = \frac{D_{is(SCIM)}}{0.62}, \quad (27)$$

$$g(SCIM) = (0.1 + 0.012 \times \sqrt[3]{P_n}), \quad (28)$$

$$D_{or(SCIM)} = D_{is(SCIM)} - g(SCIM). \quad (29)$$

The rated power is given by P_n . The determination of the number of turns per phase, W_1 , depends on the airgap flux density, $B_g(SCIM)$, and is done as follows:

$$W_1 = \frac{0.22V(SCIM)}{K_{w1} f \alpha_i \tau(SCIM) L_{st(SCIM)} B_g(SCIM)}, \quad (30)$$

where V_{SCIM} , K_{w1} , and α_i , stand for supply voltage, stator winding factor, and pole spanning coefficient, respectively. The number of conductors per slot, $n_{c(SCIM)}$, is given as:

$$n_{c(SCIM)} = \frac{\alpha_1 W_1}{p_1 q}. \quad (31)$$

A_1 represents the number of parallel current pathways. It should be noted that because a double-layer winding includes two distinct coils in each slot, an even number of slots is necessary. The definitions of the wire gauge diameter (d_{co}) and rated current (I_{in}) are as follows:

$$I_{in} = \frac{P_n}{ncos(\phi)\sqrt{3}V_{SCIM}}, \quad (32)$$

$$D_{co} = \sqrt{\frac{2I_{in}}{\pi a_p J(SCIM)}}, \quad (33)$$

where a_p , $J(SCIM)$, and η represent conductors in parallel, current density, and efficiency, respectively.

Assuming all the airgap flux passes through the stator teeth, the useful slot area, A_{su} , and stator tooth width, b_{ts} , are respectively given as:

$$A_{su} = \frac{\pi d_{co}^2 a_p n_c(SCIM)}{4K_{fill}}, \quad (34)$$

$$b_{ts} = \frac{B_g(SCIM)\tau(SCIM)}{0.96B_{ts}}. \quad (35)$$

The fill factor and stator tooth flux density are as follows K_{fill} and B_{ts} , respectively. For stator slot sizing, the lower width, b_{s1} , higher width, b_{s2} , and slot height, h_{s1} , are given as:

$$b_{s1} = \frac{\pi(D_{in(SCIM)} + 2h_{os} + 2h_w)}{N_s} - b_{ts}, \quad (36)$$

$$b_{s2} = \sqrt{4A_{su} \tan \frac{\pi}{N_s} + b_{s1}^2}, \quad (37)$$

$$h_{s2} = \frac{2A_{su}}{b_{s1} + b_{s2}}. \quad (38)$$

The lower slot height, wedge height, slot effective area, and number of stator slots are denoted as h_{os} , h_w , A_{su} , and N_s , respectively. If stator and rotor teeth give the same effects, the teeth saturation factor ($1 + K_{st}$) is calculated as follows:

$$1 + K_{st} = \frac{1 + F_{mts} + F_{mtr}}{F_{mg}}, \quad (39)$$

where F_{mts} , F_{mtr} , and F_{mg} represent stator tooth, rotor tooth, and airgap MMFs, respectively. The end-ring current, I_{er} , and magnetization current, I_{μ} , are respectively calculated as:

$$I_{er} = \frac{1b}{2\sin(\frac{\pi p_1}{N_r})}, \quad (40)$$

$$I_{\mu} = \frac{\pi p_1 (F/2)}{\sqrt[3]{2}W_1 K_{w1}}, \quad (41)$$

where I_b , N_r , and F are the rotor bar current, the number of rotor slots, and the magnetization MMF, respectively.

For the rotor slot sizing, the rotor slot pitch, τ_r , and tooth width, b_{tr} , are respectively calculated as:

$$\tau_r = \frac{\pi(D_{in(SCIM)} - 2g(SCIM))}{N_r}, \quad (42)$$

$$b_{tr} = \frac{\tau_r B_g(SCIM)}{0.96B_{tr}}. \quad (43)$$

The rotor tooth flux density is represented as B_{tr} . The rotor slot geometry is obtained by using the slot area, A_b , equation given as follows:

$$A_b = \frac{\pi}{8}(d_1^2 + d_2^2) + \frac{(d_1 + d_2)h_r}{2}. \quad (44)$$

The diameters d_1 and d_2 are obtained simultaneously from

$$d_1 = \frac{\pi(D_{re} - 2h_{or}) - N_r b_{tr}}{\pi + N_r} \text{ and } d_1 - d_2 = 2h_r \tan \frac{\pi}{N_r}. \quad (45)$$

The symbols D_{or} (SCIM), h_r , h_{cr} , and h_{or} stand for the rotor's outer diameter, rotor slot height, rotor back core height, and lower rotor slot height, respectively.

IV. Results And Discussion

The motor design parameters are shown in Table 1 and Table 2

Table 1.0: Motor Design1

Stator Parameters	Value	Rotor Parameters	Value
Slot Number	24	Rotor Bars	26
Housing Dia	255	Bar Opening [T]	1.5
Stator Lam Dia	135	Bar Opening Depth [T]	1.5
Stator Bore	135	Bar Tip Angle [T]	20
Tooth Width	2	Rotor Tooth Width [T]	4
Slot Depth	18	Bar Depth [T]	22
Slot Corner Radius	0	Bar Corner Radius [T]	1.33
Tooth Tip Depth	1	Airgap	0.3
Slot Opening	0.800045	Banding Thickness	0
Tooth Tip Angle	30	Shaft Dia	30
Sleeve Thickness	0	Shaft Hole Diameter	0.5

Table 1.2: Motor Design2

Stator Parameters	Value	Rotor Parameters	Value
Slot Number	28	Rotor Bars	36
Stator Lam Dia	245	Pole Number	4
Stator Bore	135	Bar Opening [T]	1.5
Tooth Width	2	Bar Opening Depth [T]	1.5
Slot Depth	18	Bar Tip Angle [T]	20
Slot Corner Radius	0	Rotor Tooth Width [T]	4
Tooth Tip Depth	1	Bar Depth [T]	22
Slot Opening	0.800045	Bar Corner Radius [T]	1.33
Tooth Tip Angle	30	Airgap	0.3
Sleeve Thickness	0	Banding Thickness	0

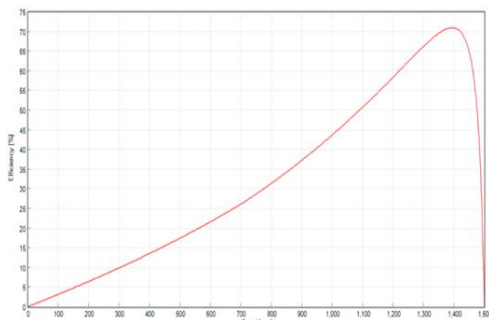


Fig.1a: Efficiency/speed motor 1

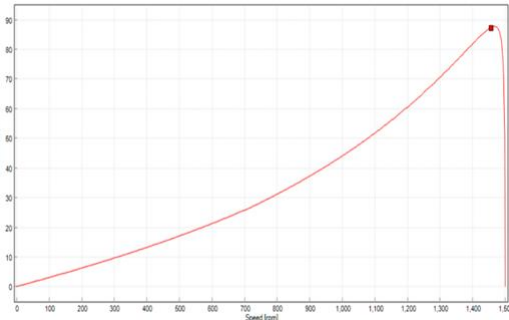


Fig. 1b: Efficiency/speed motor 2

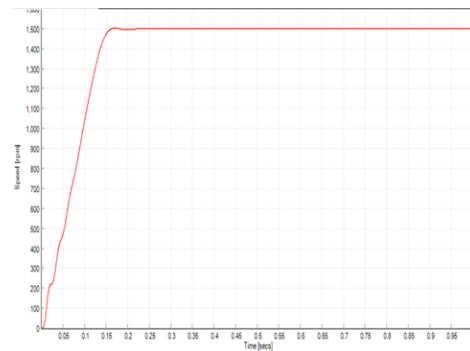


Fig.2a: Speed/Time motor 1

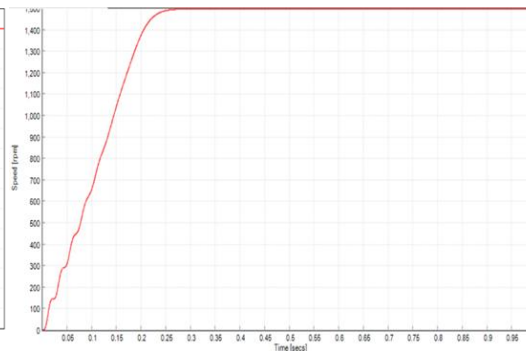


Fig.2b: Speed/Time motor 2

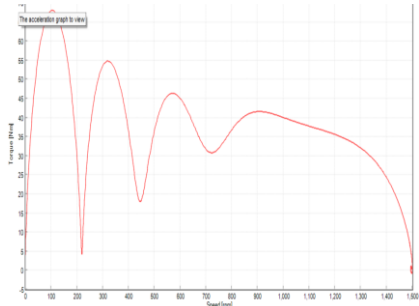


Fig.3a: Torque/Speed-motor 1

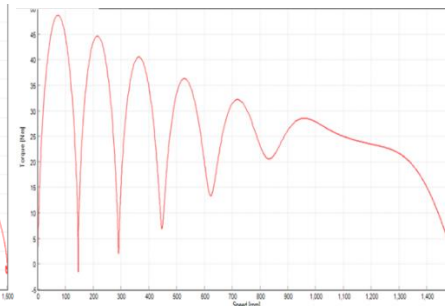


Fig.3b: Torque/Speed motor 2

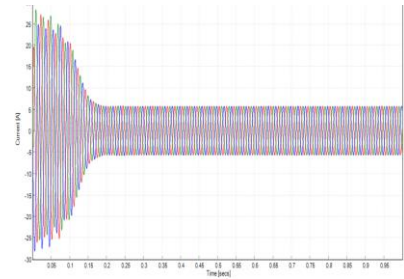


Fig.4a: Current/Time motor 1

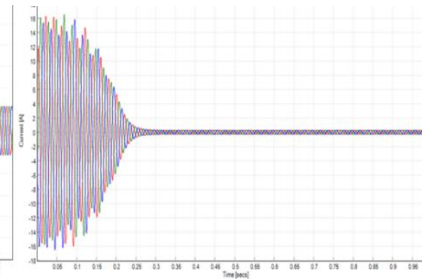


Fig.4b: Current/Time motor 2

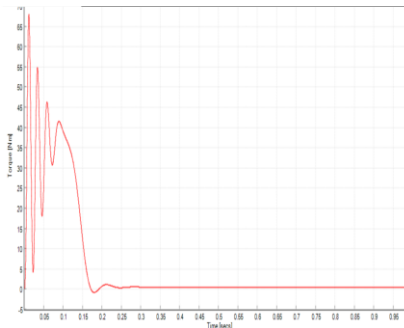


Fig.5a: Torque/Time-motor 1

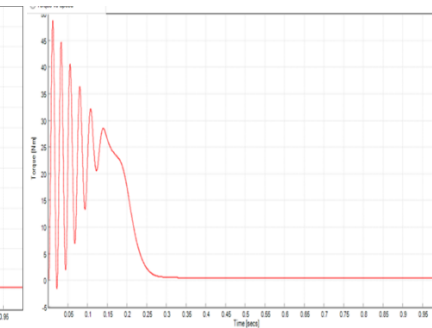


Fig.5b: Torque/Time motor 2

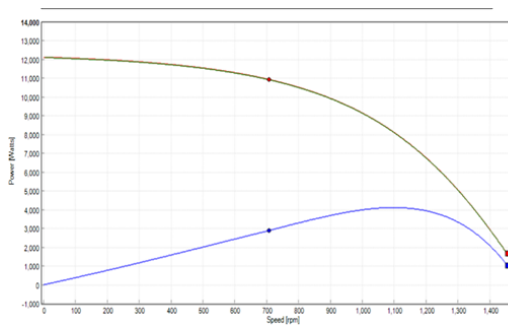


Fig.6a: Power/Speed-motor 1

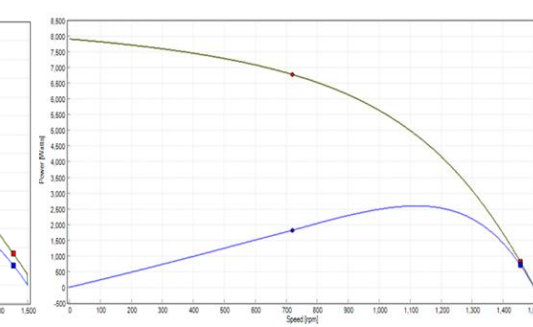


Fig.6b: Power/Speed motor 2

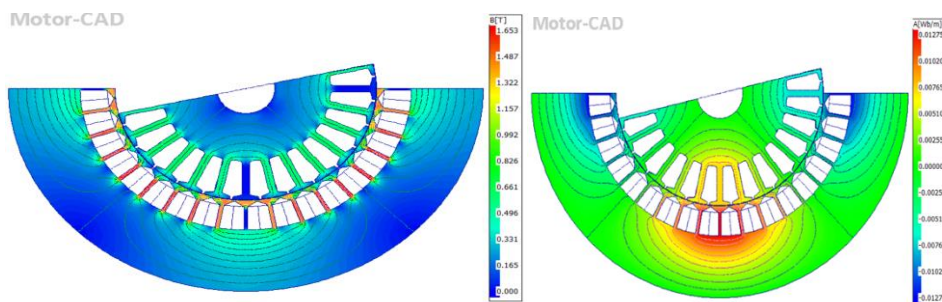


Fig.7.0: Flux lines

V. Discussion Of Results

Two motors were designed with the same parameters except the numbers of rotor and stator slots differ as shown in Table 1.0 and Table 2.0. For motor 1, the rotor and stator slot numbers are 28/36 while motor 2 has 24/26 respectively. The design and simulation were done using Motorcad version 2022. The performances of the two motors were tested, and the results are shown in the figures above, figure 1a and 1b to figure 7.0. The two motors have a reference speed of 1500rpm. Figures 1a and 1b are graphs of efficiency against speed, motor 2 has an efficiency of 88.5% while motor 1 has an efficiency of 72.8%. Figures 2a and 2b are graphs of speed against time, motor 1 has a better speed settling time of 0.15sec, whereas motor 2 settling time is at 0.25sec. Graphs of torque against speed are shown in Figures 3a and 3b. Motor 1 has a higher starting torque of 68.5Nm while motor 2 has a starting torque of 48.5Nm both at the speed of 100rpm. The graphs of currents against time are shown in Figures 4a and 4b. Motor 1 has a starting current of 30Amps and a settling time of 0.15sec while motor 2 has a starting current of 16Amps and a settling time of 0.225sec. Figures 5a and 5b are graphs of torque against time. Motor 1 has a starting torque of 68Nm at settling of 0.0025sec while motor 2 has a starting torque of 48.5Nm at settling time of 0.25sec. Figures 6a and 6b are the graphs of power against speed. Motor 1 has a capacity of 12,000W while motor 2 has a capacity of 8,000W. Figures 7a and 7b are the graphs of flux lines of the design motor showing the hot spot in terms of its density and potential. The motor's cost and manufacturability may be affected by the number of slots. Specialized manufacturing methods may be needed for complex slot designs, which would raise production costs. As a result, designers must balance manufacturing sustainability with performance requirements. The number of slots can affect the motor's acceleration, speed regulation, and beginning torque, among other operating properties. For transportation applications, smooth motor starting and operation can be ensured through proper slot design.

VI. Conclusion

The effect of rotor slot numbers on motor efficiency is complex. While additional slots can result in stronger starting torque and lower torque ripple, they can also result in larger copper losses due to increased rotor resistance. As a consequence of this, depending on the precise design and operating conditions, efficiency varies. An incorrect stator slot count can cause magnetic saturation, resulting in increased iron losses and motor overheating. The stator slot number can affect the motor's beginning performance, including starting torque and current drawn during startup. A higher slot count can result in stronger starting qualities. Designing a motor for a higher efficiency required a better selection of the motor's parameters. Thus, this work is recommended to motor manufacturers, system engineers, and production Engineers, especially those that require a higher efficiency and better output. An induction motor's rotor and stator slot numbers are chosen for transportation-related reasons, and this choice has a significant impact on the motor's efficiency, dependability, and manufacturability. These elements can be optimally balanced by proper slot design to satisfy the unique needs of transportation networks, guaranteeing dependable, streamlined operation.

References

- [1] Gyftakis, Konstantinos N., And Joya Kappatou. "The Impact Of The Rotor Slot Number On The Behavior Of The Induction Motor." *Advances In Power Electronics* 2013
- [2] Babypriya, B., & Gomathi, S. Numerical Analysis On Impact Of Choice Of Number Of Rotor Slots On Performance Of Three Phase Induction Motor. *Materials Today: Proceedings*, 45, 2364-2370 2021
- [3] Gundogdu, T., Z. Q. Zhu, And J. C. Mipo. "Influence Of Rotor Slot Number On Rotor Bar Current Waveform And Performance In Induction Machines." In 2017 20th International Conference On Electrical Machines And Systems (Icems), Pp. 1-6. Ieee, 2017.
- [4] Mach, Martin, Radoslav Cipin, Marek Toman, And Vitezslav Hajek. "Impact Of Number Of Rotor Slots On Performance Of Three-Phase And Single-Phase Induction Machines." In 2018 Ieee International Conference On Environment And Electrical Engineering And 2018 Ieee Industrial And Commercial Power Systems Europe (Eeeic/I&Cps Europe), Pp. 1-6. Ieee, 2018.
- [5] Valtonen, M., A. Parviainen, And J. Pyrhonen. "The Effects Of The Number Of Rotor Slots On The Performance Characteristics Of Axial-Flux Aluminium-Cage Solid-Rotor Core Induction Motor." In 2007 Ieee International Electric Machines & Drives Conference, Vol. 1, Pp. 668-672. Ieee, 2007.
- [6] Okoro, O. I., Abunike, C. E., Akuru, U. B., Awah, C. C., Udenze, P. I., & Innocent, U. O. (2022). Electromagnetic Performance Characterization Of 4-Pole Squirrel-Cage Motors With Different Rotor Slot Combinations. In 2022 4th International Conference On Emerging Trends In Electrical, Electronic And Communications Engineering (Elecom) (Pp. 1-6). Mauritius. Doi:10.1109/Elecom54934.2022.9965228
- [7] Okoro, O.I. (2004). A Modelling Technique For Accurate Simulation Of Squirrel-Cage Induction Machine With Deep Rotor Bars. *Nse Technical Transactions*, Vol. 39, No. 2, Pp. 35-49.
- [8] Aho, Tuomo, Janne Nerg, And J. Pyrhonen. "The Effect Of The Number Of Rotor Slits On The Performance Characteristics Of Medium-Speed Solid Rotor Induction Motor." (2006): 515-519.
- [9] Nandi, Subhasis. "Modeling Of Induction Machines Including Stator And Rotor Slot Effects." In 38th Ias Annual Meeting On Conference Record Of The Industry Applications Conference, 2003., Vol. 2, Pp. 1082-1089. Ieee, 2003.
- [10] Maloma, Evelin, Mbika Muteba, And Dan-Valentin Nicolae. "Effect Of Rotor Bar Shape On The Performance Of Three Phase Induction Motors With Broken Rotor Bars." In 2017 International Conference On Optimization Of Electrical And Electronic Equipment (Optim) & 2017 Intl Aegean Conference On Electrical Machines And Power Electronics (Acemp), Pp. 364-369. Ieee, 2017.
- [11] Akhtar, Mohammad Junaid, And Ranjan Kumar Behera. "Optimal Design Of Stator And Rotor Slot Of Induction Motor For Electric Vehicle Applications." *Iet Electrical Systems In Transportation* 9, No. 1 (2019): 35-43. Lavanya, M., P. Selvakumar, S. Vijayshankar,

- And C. Easwarlal. "Performance Analysis Of Three Phase Induction Motor Using Different Magnetic Slot Wedges." In 2014 Ieee 2nd International Conference On Electrical Energy Systems (Icees), Pp. 164-167. Ieee, 2014.
- [12] Elhaija, W. Abu, V. Ghorbanian, J. Faiz, And H. Nejadi-Koti. "Significance Of Rotor Slots Number On Induction Motor Operation Under Broken Bars." In 2017 Ieee International Electric Machines And Drives Conference (Iemdc), Pp. 1-8. Ieee, 2017.
- [13] Joksimović, Gojko, Emil Levi, Aldin Kajević, Mario Mezzarobba, And Alberto Tassarolo. "Optimal Selection Of Rotor Bar Number For Minimizing Torque And Current Pulsations Due To Rotor Slot Harmonics In Three-Phase Cage Induction Motors." Ieee Access 8, 228572-228585, 2020.
- [14] Naderi, Peyman, And Ali Taheri. "Slot Numbering And Distributed Winding Effects Analysis On The Torque/Current Spectrum Of Three-Phase Wound-Rotor Induction Machine Using Discrete Modeling Method." Electric Power Components And Systems 43, No. 15 (2015): 1717-1726.
- [15] Boglietti, A., Bojoi, R.I., Cavagnino, A., Guglielmi, P. And Miotto, A., 2012. Analysis And Modeling Of Rotor Slot Enclosure Effects In High-Speed Induction Motors. Ieee Transactions On Industry Applications, 48(4), Pp.1279-1287, 2019.
- [16] Abdel-Khalik, A.S., Massoud, A. And Ahmed, S., Standard Three-Phase Stator Frames For Multiphase Machines Of Prime-Phase Order: Optimal Selection Of Slot/Pole Combination. Ieee Access, 7, Pp.78239-78259.
- [17] Zhang, D., Park, C.S. And Koh, C.S., A New Optimal Design Method Of Rotor Slot Of Three-Phase Squirrel Cage Induction Motor For Nema Class D Speed-Torque Characteristic Using Multi-Objective Optimization Algorithm. Ieee Transactions On Magnetics, 48(2), Pp.879-882, 2012.
- [18] Zhang, Dianhai, Chang Soon Park, And Chang Seop Koh. "A New Optimal Design Method Of Rotor Slot Of Three-Phase Squirrel Cage Induction Motor For Nema Class D Speed-Torque Characteristic Using Multi-Objective Optimization Algorithm." Ieee Transactions On Magnetics 48, No. 2: 879-882, 2012.
- [19] Niazazari, M., M. Mirsalim, And S. Mohamadi. "Effect Of Rotor Slots Parameters On Synchronization Capability Of Slotted Solid Rotor Line Start Permanent Magnet Motor." In 4th Annual International Power Electronics, Drive Systems And Technologies Conference, Pp. 60-65. Ieee, 2013.
- [20] Juhaniya, Ahamed Ibrahim Sithy, Asrul Ibrahim Ahmad, Muhammad Ammirul Atiqi Mohd Zainuri, And Mohd Asyraf Zulkifley. "An Analytical Model Of Induction Motors For Rotor Slot Parametric Design Performance Evaluation." International Journal Of Advanced Computer Science And Applications 13, No. 12, 2022.
- [21] Chen, J. T., Z. Q. Zhu, S. Iwasaki, And Rajesh P. Deodhar. "Influence Of Slot Opening On Optimal Stator And Rotor Pole Combination And Electromagnetic Performance Of Switched-Flux Pm Brushless Ac Machines." Ieee Transactions On Industry Applications 47, No. 4 (2011): 1681-1691.
- [22] Okoro, O. I. (2004). Steady-State Analysis Of Squirrel-Cage Induction Machine With Skin-Effect, Akamai University Pacific Journal Of Science And Technology, No.5, Vol. 2, Pp.56-62.
- [23] Paredes, Jesús, Borja Prieto, Marco Satrústegui, Ibón Elósegui, And Patxi González. "Improving The Performance Of A 1-Mw Induction Machine By Optimally Shifting From A Three-Phase To A Six-Phase Machine Design By Rearranging The Coil Connections." Ieee Transactions On Industrial Electronics 68, No. 2 1035-1045. 2020
- [24] Chiweta E. Abunike, Udochukwu B. Akuru, Ogbonnaya I. Okoro And Chukwuemeka C. Awah (2023) Sizing, Modeling, And Performance Comparison Of Squirrel-Cage Induction And Wound-Field Flux Switching Motors. Mathematics 2023, 11(16), 3596; <https://doi.org/10.3390/Math11163596>